

Supplemental information

**Prox2 and Runx3 vagal sensory neurons
regulate esophageal motility**

Elijah D. Lowenstein, Pierre-Louis Ruffault, Aristotelis Misios, Kate L. Osman, Huimin Li, Rachel S. Greenberg, Rebecca Thompson, Kun Song, Stephan Dietrich, Xun Li, Nikita Vladimirov, Andrew Woehler, Jean-François Brunet, Niccolò Zampieri, Ralf Kühn, Stephen D. Liberles, Shiqi Jia, Gary R. Lewin, Nikolaus Rajewsky, Teresa E. Lever, and Carmen Birchmeier

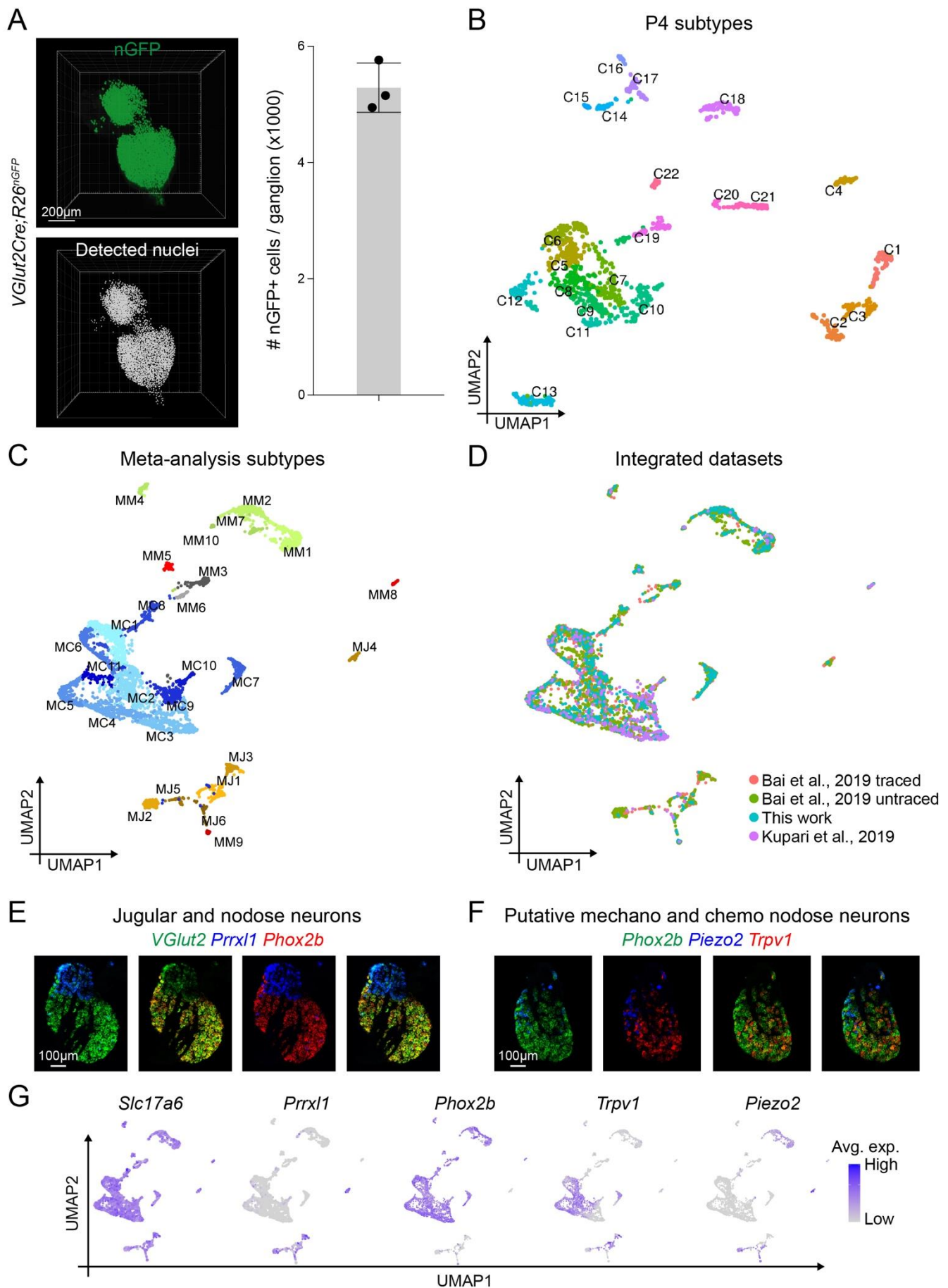


Figure S1. scRNAseq analysis assigns a developmental origin and putative function to vagal neuron subtypes, related to Figure 1. (A) Lightsheet imaging of a vagal ganglion from a *VGlut2^{Cre};R26^{nGFP}* mouse at P4; GFP+ neuronal nuclei (green, **top**), and all detected nuclei (gray, **bottom**) are shown. Detected nuclei were quantified using IMARIS v9.9.0 (5288±423 nuclei per ganglion, n=3). **(B)** UMAP plot based on single cell RNA-seq data from 1392 neurons isolated at P4 from *VGlut2^{Cre};R26^{nGFP}* animals revealed 22 subtypes (color coded and numbered). **(C)** UMAP plot based on the meta-analysis of 4,442 neurons revealed 27 subtypes (color coded and numbered, *Meta-Jugular* (MJ) 1-6, *Meta-Chemo* (MC) 1-11, *Meta-Mechano* (MM) 1-10). **(D)** UMAP plot based on the meta-analysis displaying cells of each data set by separate colors; all data sets contributed cells to each subtype. **(E)** smFISH showing that all vagal neurons are *VGlut2*+ (*Slc17a6*); they express *Prrxl1* or *Phox2b* that distinguish jugular and nodose ganglia, respectively. **(F)** smFISH showing that nodose neurons (*Phox2b*+) express *Piezo2* or *Trpv1* that mark putative mechanosensory and chemosensory neurons, respectively. **(G)** UMAP plots for *VGlut2* (*Slc17a6*), *Prrxl1*, *Phox2b*, *Trpv1* and *Piezo2*. Data in A are represented as mean ± SD. Images in **(E, F)** were stitched using the tile-scan mode.

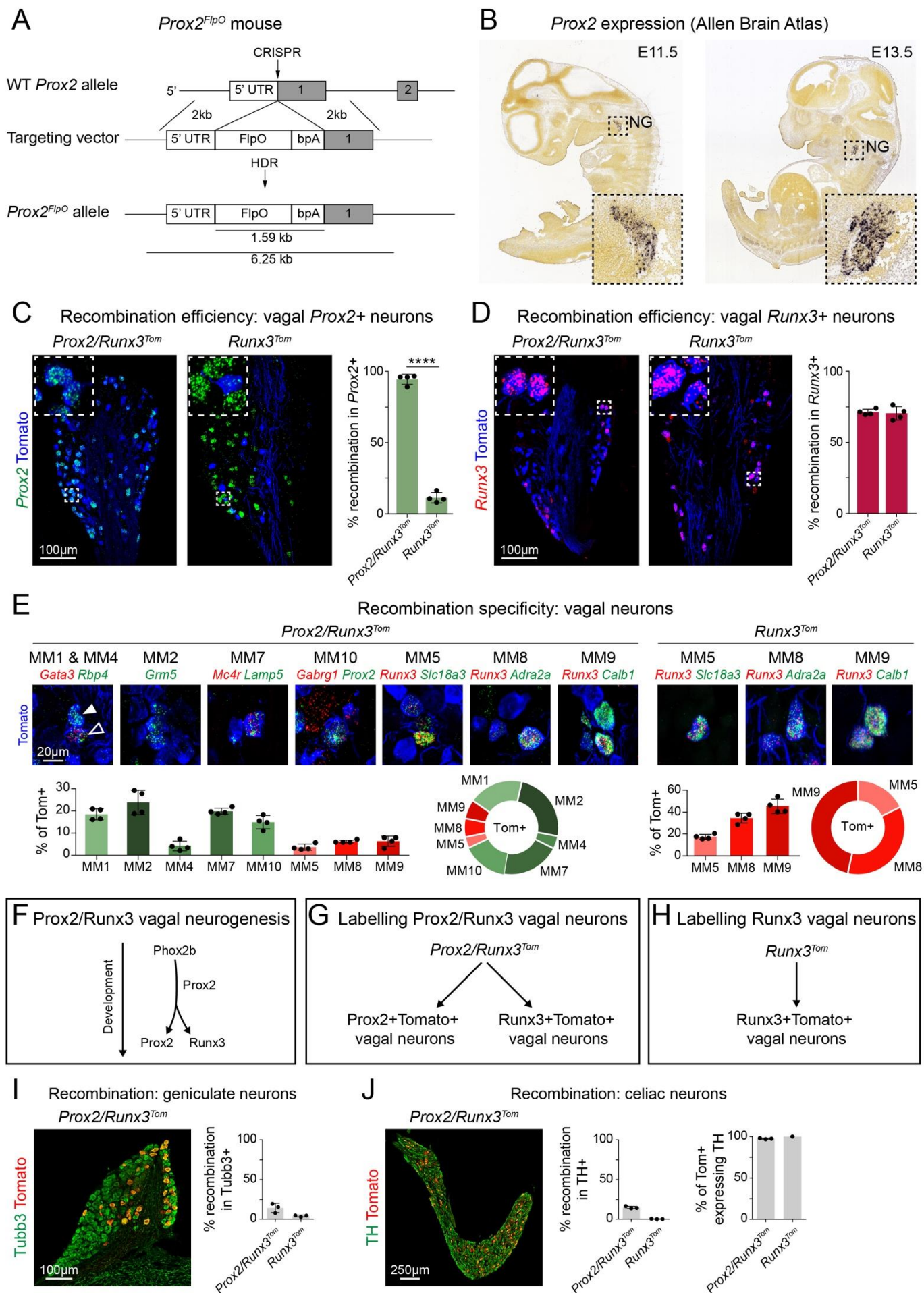


Figure S2. Generation and characterization of the *Prox2^{FlpO}* mouse strain, related to Figure 2. (A) Scheme showing the strategy used to generate the *Prox2^{FlpO}* allele. (B) *In situ* hybridizations against *Prox2* mRNA in sagittal sections of E11.5 (left) and E13.5 (right) embryos; images were obtained from the Allen Brain Atlas (<https://developingmouse.brain-map.org/>). (C) Recombination efficiency in *Prox2*⁺ neurons in *Prox2/Runx3^{Tom}* (*Prox2^{FlpO};Phox2b^{Cre};Ai65*) (left) and *Runx3^{Tom}* (*Runx3^{Cre};Prox2^{FlpO};Ai65*) (right) animals determined by smFISH analysis of *Prox2* (green) and immunohistological analysis of tdTomato expressing cells (blue). Quantifications are indicated, n=4. (D) Recombination efficiency in *Runx3*⁺ neurons in *Prox2/Runx3^{Tom}* (left) and *Runx3^{Tom}* (right) animals determined by smFISH analysis of *Runx3* (red) and immunohistological analysis of tdTomato expressing cells (blue). Quantifications are indicated below, n=4. (E) smFISH images from *Prox2/Runx3^{Tom}* (left) animals showing recombination in *Prox2*⁺ (green) and *Runx3*⁺ (red) neuronal subtypes. smFISH images from *Runx3^{Tom}* (right) animals showing recombination in *Runx3*⁺ (red) subtypes. Quantifications are indicated below, n=4. (F) Putative lineage relationships between *Prox2* and *Runx3* neurons. We propose that *Runx3*⁺ neurons have a history of *Prox2* expression and are therefore labelled in *Runx3^{Cre};Prox2^{FlpO};Ai65* mice. (G) Strategy used to label *Prox2* and *Runx3* vagal neurons with tdTomato using *Prox2/Runx3^{Tom}* (*Prox2^{FlpO};Phox2b^{Cre};Ai65*) mice. (H) Strategy used to label *Runx3* vagal neurons with tdTomato using *Runx3^{Tom}* (*Runx3^{Cre};Prox2^{FlpO};Ai65*) mice. (I) Immunohistological analysis (left) using tdTomato (red) and *Tubb3* (green) antibodies shows recombination in geniculate neurons of a *Prox2/Runx3^{Tom}* animal. Quantifications (right) of recombination in *Prox2/Runx3^{Tom}* and *Runx3^{Tom}* mice, respectively, n=3. (J) Immunohistological analysis (left) using tdTomato (red) and TH (green) antibodies shows recombination in celiac neurons of a *Prox2/Runx3^{Tom}* animal. Quantifications (right) of recombination in celiac TH⁺ neurons, and of TH expression in recombined (tdTomato⁺) neurons in *Prox2/Runx3^{Tom}* and *Runx3^{Tom}* mice, respectively, n=3. Only a third of *Runx3^{Tom}* mice showed any recombined celiac neurons, and these were all TH⁺. Data are represented as mean ± SD, ****p < 0.0001, unpaired two-tailed t-test. Images in (C, D, I, J) were stitched using the tile-scan mode.

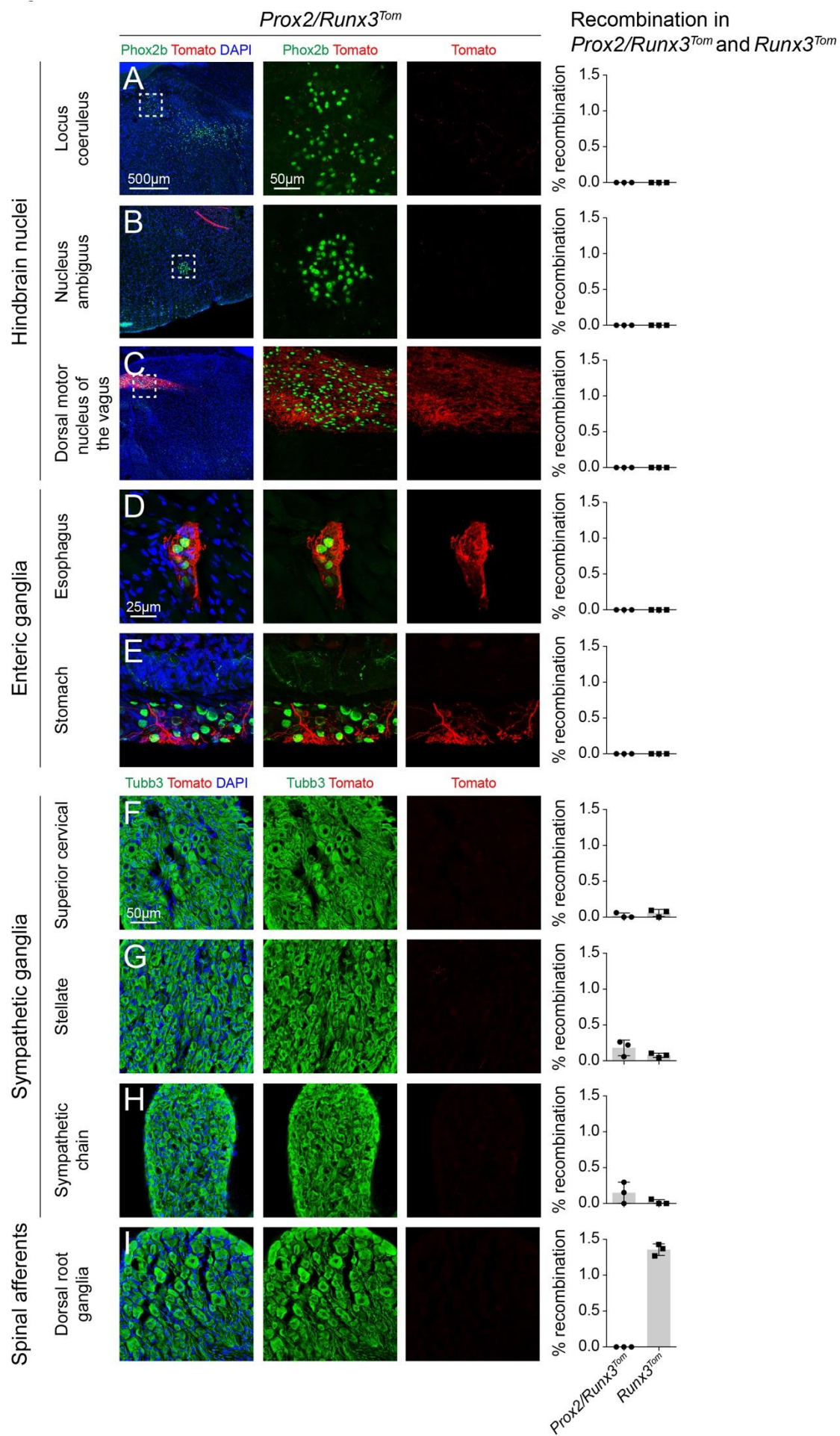


Figure S3. Recombination in *Prox2/Runx3^{Tom}* and *Runx3^{Tom}* animals, related to Figure 2. (A-E) Immunohistological analysis using antibodies against Phox2b (green) and tdTomato (red) of the **(A)** locus coeruleus, **(B)** nucleus ambiguus, **(C)** dorsal motor nucleus of the vagus, **(D)** esophageal enteric ganglia and **(E)** stomach enteric ganglia in *Prox2/Runx3^{Tom}* animals; DAPI (blue) was used as a counterstain. Quantifications **(right)** of recombination in Phox2b+ in *Prox2/Runx3^{Tom}* and *Runx3^{Tom}* mice, respectively, n=3. **(F-I)** Immunohistological analysis using antibodies against Tubb3 (green) and tdTomato (red) of the **(F)** superior cervical, **(G)** stellate, **(H)** sympathetic chain, and **(I)** dorsal root ganglia in *Prox2/Runx3^{Tom}* mice; DAPI (blue) was used as a counterstain. Quantifications **(right)** of recombination in Tubb3+ cell in *Prox2/Runx3^{Tom}* or *Runx3^{Tom}* mice n=3. Data are represented as mean \pm SD.

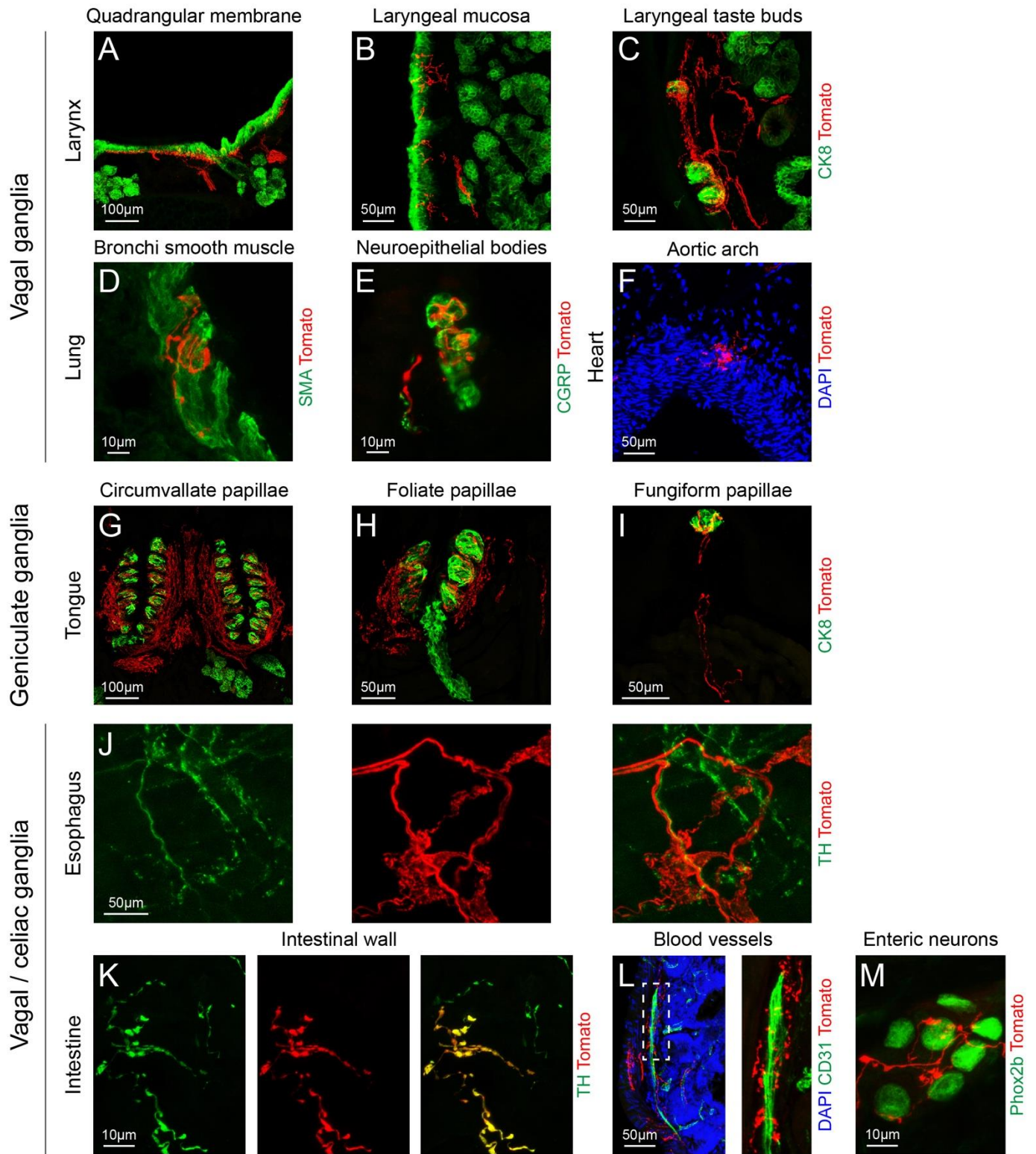


Figure S4. Innervation targets of *Prox2/Runx3* neurons, related to Figure 2. (A-C) Immunohistological analysis using Ck8 (green) and tdTomato (red) antibodies shows vagal tdTomato+ innervation of the **(A)** quadrangular membrane of the larynx, **(B)** laryngeal mucosa, and **(C)** laryngeal taste buds. **(D)** Immunohistological analysis using SMA (green) and tdTomato (red) analysis shows vagal tdTomato+ innervation of smooth muscle cells of bronchi in the lung. **(E)** Immunohistological analysis using antibodies against CGRP (green) and tdTomato (red) shows vagal tdTomato+ innervation of neuroepithelial bodies in the lung. **(F)** Immunohistological analysis using tdTomato (red) antibodies shows vagal tdTomato+ innervation of the aortic arch; DAPI (blue) was used as a counterstain. **(G-I)** Immunohistological analysis using antibodies against Ck8 (green) and tdTomato (red) shows geniculate tdTomato+ innervation of **(H)** circumvallate, **(I)** foliate, and **(J)** fungiform papillae. **(J,K)** Immunohistological analysis using antibodies against TH (green) and tdTomato (red) shows the absence of axons co-expressing TH and tdTomato in the esophagus, but extensive co-expression in the intestine. **(L)** Immunohistological analysis using antibodies against CD31 (green) and tdTomato (red) shows endings on blood vessels in the intestine. **(M)** Immunohistological analysis using antibodies against Phox2b (green) and tdTomato (red) shows varicose endings on enteric ganglia in the intestine. Images in (A, G, H, J, K, L) were stitched using the tile-scan mode.

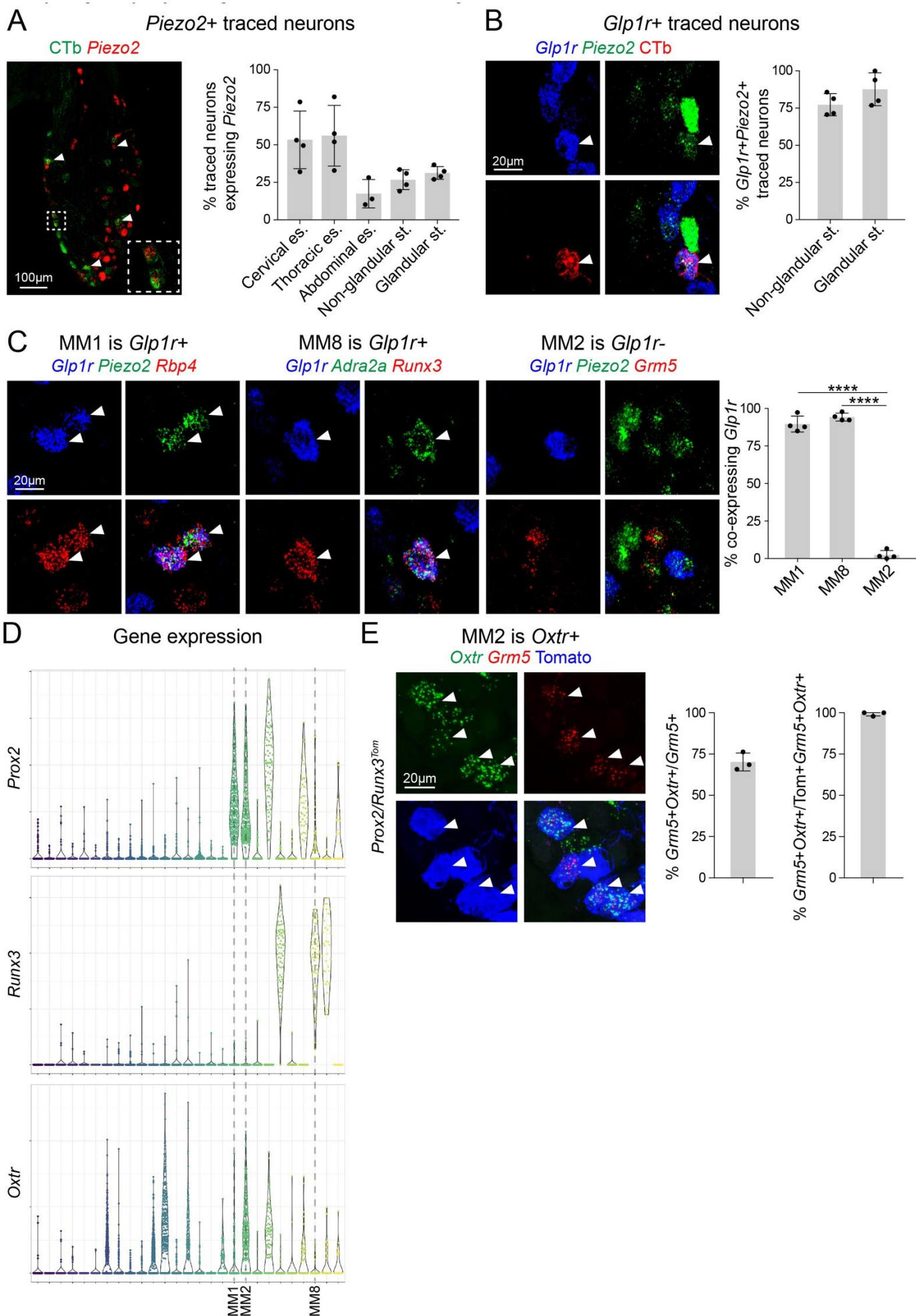


Figure S5. MM1 and MM8 include *Glp1r*+ stomach projecting neurons, MM2 include *Oxtr*+ esophageal projecting neurons, related to Figure 3. (A) smFISH (left) analysis of the vagal ganglion using a *Piezo2* (red) probe, combined with an immunohistological analysis of CTb (green) after CTb injection into the glandular stomach. (Right) Quantification of *Piezo2*+ neurons identified after CTb or Fast Blue injection into various sites of the upper gastrointestinal tract, n=3–4. Neurons from the cervical and thoracic esophagus were traced using Fast Blue at P7, and neurons from the abdominal esophagus, non-glandular and glandular stomach were traced using CTb in adults. (B) smFISH analysis of the vagal ganglion (left) using *Piezo2* (green) and *Glp1r* (blue) probes, combined with immunohistological analysis of CTb (red) after CTb injection into the stomach. The quantification after injection into the glandular and non-glandular is shown on the right; n=4. (C) smFISH analysis (left) of *Glp1r* expression in MM1 (probes: *Piezo2* in green, *Rbp4* in red, and *Glp1r* in blue, left), MM8 (probes: *Adra2a* in green, *Runx3* in red, and *Glp1r* in blue, middle) and MM2 (probes: *Piezo2* in green, *Grm5* in red, and *Glp1r* in blue. The quantification of the proportions of MM1, MM8 and MM2 neurons expressing *Glp1r* is shown on the right, n=4. (D) Violin plots for *Prox2*, *Runx3* and *Oxtr* expression derived from the meta-analysis. MM1, MM2 and MM8 subtypes are indicated. (E) smFISH analysis using (left) of *Oxtr* (green) and *Grm5* (red) probes, combined with immunohistological analysis using tdTomato antibodies (blue). Among the *Prox2*/*Runx3* neuronal subtypes, only MM2 expresses *Grm5*. The quantifications of MM2 neurons (*Grm5*+) expressing *Oxtr*, and of recombined *Oxtr*+ MM2 (*Grm5*+) neurons (i.e. tdTomato+) in *Prox2*/*Runx3*^{Tom} animals is shown on the right, n=3. Data are represented as mean \pm SD, **p < 0.0001, unpaired two-tailed t-test (B), Ordinary one-way ANOVA with Tukey's multiple comparisons test (C). Image in (A) was stitched using the tile-scan mode.**

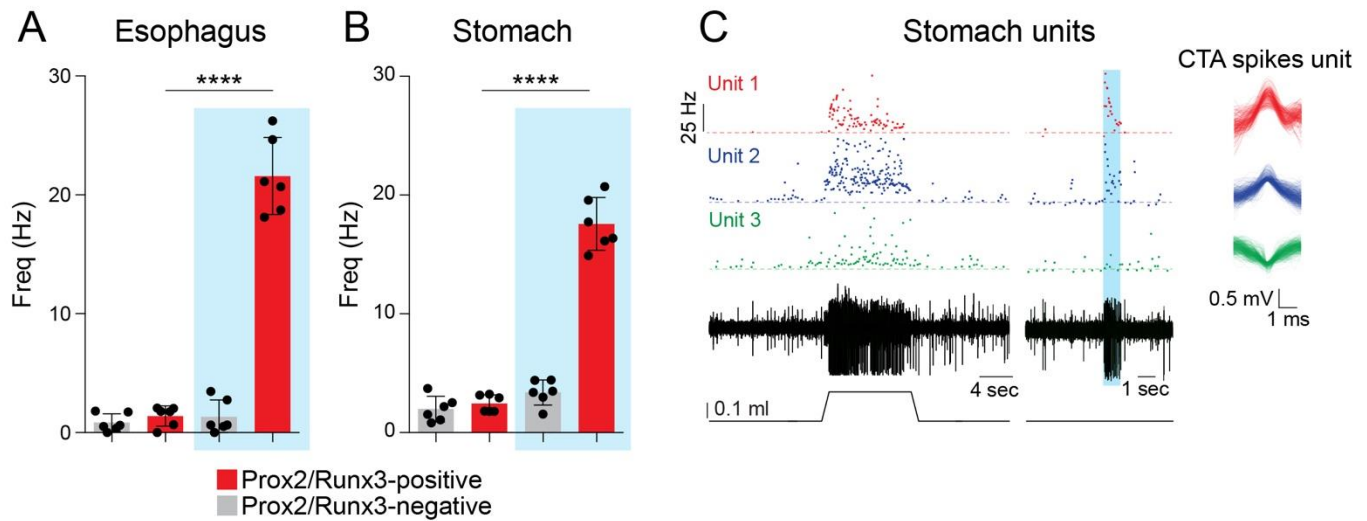


Figure S6. Optogenetic activation of Prox2/Runx3 mechanoreceptors, related to Figure 4. **(A,B)** Quantification of the firing properties of Prox2/Runx3-positive (red, light-sensitive) and Prox2/Runx3-negative (gray, light-insensitive) single fibers. Action potential firing frequency (Hz) was measured on single esophageal **(A)** or stomach **(B)** fibers from *Prox2/Runx3^{ChR}* (*Prox2^{FlpO};Phox2b^{Cre};Ai80*) animals with and without blue light stimulation (indicated in blue shading). Under light stimulation, Prox2/Runx3-positive units dramatically increased their firing frequency; $n=6$. **(C)** Spike sorting identified three individual mechanosensitive units (shown in red, blue and green) present in a single fiber. Points form a raster plot of single unit instantaneous firing frequencies after stomach distention (**left**, 0.3 ml stimuli, the black line underneath the plot displays the change in stomach volume), or light activation (indicated by blue shading). Note that units 1 and 2 (red and blue) are light-sensitive and thus Prox2/Runx3-positive, whereas the light insensitive unit 3 (green) is Prox2/Runx3-negative. Cycle trigger average (CTA) of 500 spikes (**right**) of the 3 units identified in this fiber after stomach distention. Data are represented as mean \pm SD, **** $p < 0.0001$, Ordinary one-way ANOVA with Tukey's multiple comparisons test.

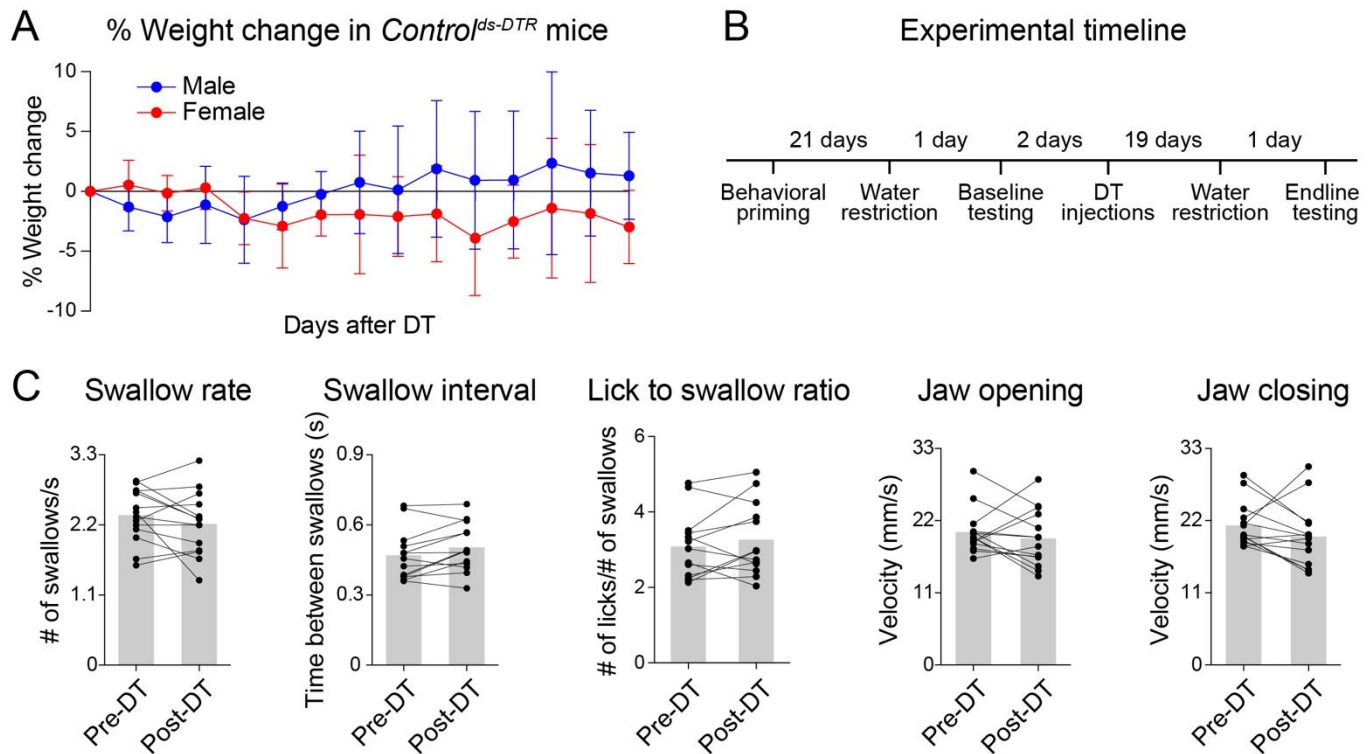


Figure S7. Oropharyngeal swallow-related behaviors that were not affected by ablation of Prox2/Runx3 neurons, related to Figure 5. (A) Graph showing weight change in *Control*^{ds-DTR} (*Prox2*^{FlpO}; *Tau*^{ds-DTR}) control mice over 14 days after DT administration. **(B)** Outline of the experimental timeline. **(C)** Many oropharyngeal swallow-related behaviors were not affected after ablation of Prox2/Runx3 neurons. Swallow rate, swallow interval, lick to swallow ratio, jaw opening and closing velocity were unaffected, n=13-14. Data are represented as mean \pm SD, paired two-tailed t-test.